BBA - Proteins and Proteomics 1867 (2019) 595–603

Contents lists available at ScienceDirect

BBA - Proteins and Proteomics

journal homepage: www.elsevier.com/locate/bbapap

Characterization of a novel cytochrome c_{GJ} as the electron acceptor of XoxF-MDH in the thermoacidophilic methanotroph *Methylacidiphilum fumariolicum* SolV

Wouter Versantvoort[a], Arjan Pol[a], Lena J. Daumann[b], James A. Larrabee[c], Aidan H. Strayer[c], Mike S.M. Jetten[a], Laura van Niftrik[a], Joachim Reimann[a], Huub J.M. Op den Camp[a,*]

[a] Department of Microbiology, IWWR, Radboud University, Heyendaalseweg, 135 6525, AJ, Nijmegen, the Netherlands
[b] Ludwig-Maximilians-Universität München, Department Chemie, Butenandtstr. 5-13, 81377 München, Germany
[c] Department of Chemistry and Biochemistry, Middlebury College, Middlebury, VT, USA

ARTICLE INFO

Keywords:
Cytochrome c_{GJ}
Methylotrophy
Verrucomicrobia
Acidophile
Methanol dehydrogenase
Cytochrome
Electron transfer
Heme
Metalloprotein

ABSTRACT

Methanotrophs play a prominent role in the global carbon cycle, by oxidizing the potent greenhouse gas methane to CO_2. Methane is first converted into methanol by methane monooxygenase. This methanol is subsequently oxidized by either a calcium-dependent MxaF-type or a lanthanide-dependent XoxF-type methanol dehydrogenase (MDH). Electrons from methanol oxidation are shuttled to a cytochrome redox partner, termed cytochrome c_L. Here, the cytochrome c_L homolog from the thermoacidophilic methanotroph *Methylacidiphilum fumariolicum* SolV was characterized. SolV cytochrome c_{GJ} is a fusion of a XoxG cytochrome and a periplasmic binding protein XoxJ. Here we show that XoxGJ functions as the direct electron acceptor of its corresponding XoxF-type MDH and can sustain methanol turnover, when a secondary cytochrome is present as final electron acceptor. SolV cytochrome c_{GJ} (XoxGJ) further displays a unique, red-shifted absorbance spectrum, with a Soret and Q bands at 440, 553 and 595 nm in the reduced state, respectively. VTVH-MCD spectroscopy revealed the presence of a low spin iron heme and the data further shows that the heme group exhibits minimal ruffling. The midpoint potential $E_{m,pH7}$ of +240 mV is similar to other cytochrome c_L type proteins but remarkably, the midpoint potential of cytochrome c_{GJ} was not influenced by lowering the pH. Cytochrome c_{GJ} represents the first example of a cytochrome from a strictly lanthanide-dependent methylotrophic microorganism.

1. Introduction

Both aerobic and anaerobic methanotrophs play an important role in the global carbon cycle by oxidizing the greenhouse gas methane to CO_2. Methane is mainly produced in anoxic environments through the anaerobic degradation of biomass by methanogenic archaea [1]. Before reaching the atmosphere, methane can be used as an electron donor by various microorganisms, which couple its oxidation to the reduction of nitrite, nitrate, metal-oxides, sulfate and oxygen [2–9]. Aerobic methanotrophs, with representatives in the Alpha- and Gammaproteobacteria [10] and Verrucomicrobia [11] have been intensely studied and are widespread in nature, from lakes sediment and peatlands to more extreme environments as permafrost and volcanic mudpots [12]. The first step in their metabolism is the oxygen-dependent activation of methane into methanol by methane monooxygenase [13]. Methanol is subsequently oxidized to formaldehyde by methanol dehydrogenase (MDH). MDH is quinoprotein with a pyrroloquinoline quinone (PQQ) prosthetic group. Formaldehyde can either be oxidized to formate and eventually CO_2 or be assimilated into biomass via the RuMP or serine pathway. Instead of assimilation of formaldehyde, some methanotrophs utilize the Calvin-Benson-Bassham cycle for carbon fixation [4,11,12,14,15].

Methanol oxidation to formaldehyde was long believed to be solely catalyzed by the well-characterized calcium-dependent MDH (MxaFI) [16]. However, recent studies have identified an alternative MDH (XoxF), which is lanthanide-dependent [17–20]. These XoxF-type MDHs are widespread in nature and can be classified into multiple phylogenetic clades [21]. The same holds true for the physiological

Abbreviations: MDH, Methanol dehydrogenase; ICP-MS, Inductively Coupled Plasma Mass Spectrometry; MMO, Methane monooxygenase; VTVH-MCD, variable temperature variable field magnetic circular dichroism

* Corresponding author.
E-mail address: h.opdencamp@science.ru.nl (H.J.M. Op den Camp).

https://doi.org/10.1016/j.bbapap.2019.04.001
Received 15 January 2019; Received in revised form 28 March 2019; Accepted 2 April 2019
Available online 04 April 2019

electron acceptor of MDH, cytochrome c_L (MxaG/XoxG), which is usually encoded in the *mxa* or *xox* operon (21). XoxG cytochromes are very divergent and can be clustered into four distinct clades [22]. Regardless of their diversity, the primary function of these cytochromes is most likely the same i.e. accept electrons from methanol oxidation by MDH and shuttle them to the next partner in the electron transfer chain.

The role as dedicated electron acceptor of MDH was first shown for the Mxa-type. Here cytochrome c_L accepted electrons from MDH and donated them to cytochrome c_H, which in its turn donated electrons to a terminal oxidase [23]. More recently, XoxG has been shown to function as the dedicated electron acceptor of XoxF MDH [24]. However, it was not clear how the electrons were subsequently transferred. The so far characterized cytochrome c_L's contain one high potential, covalently bound, low-spin heme group with a His-Met coordinated iron [23]. The ferrous form shows typical absorption peaks around 550 nm for the α-band and 415 for the Soret region. Besides these more typical *c*-type cytochrome features, cytochrome c_L has an unusual large size (17–21 kDa), is able to react with carbon monoxide and both heme propionates are solvent exposed [23–26]. Cytochrome c_L proteins have no sequence similarity to any other cytochrome. The sequence is unique with only the haem binding site CxxCH shared with all other cytochromes c. But remarkably, the 3D structures are very similar, with 3 large α-helices forming a haem cleft.

Another gene usually present in the MDH operon is MxaJ/XoxJ [21]. Recently, the MxaJ structure of *M. aminisulfidivorans* MP was resolved, which showed a "bi-lobate" folding architecture found in periplasmic binding proteins [27]. MxaJ might be involved in protein binding, rather than binding small molecules and could stabilize the interaction between MDH and pMMO or assist in conformational changes in MDH and cytochrome c_L to bring the PQQ and heme group close enough for efficient electron transfer [27–30]. MxaJ has been copurified with MDH in *Acetobacter methanolicus* and *M. aminisulfidivorans* MP^T, where it lowered V_{max} and increased K_m in the former but increased V_{max} and lowered K_m in the latter during enzyme assays [29,30]. MxaJ deletion mutants of *Paracoccus denitrificans* were unable to grow on methanol and did not have any MDH activities in whole cells, indicating the importance of MxaJ for the formation of active MDH [28].

Methylacidiphilum fumariolicum SolV is a thermoacidophilic methanotroph first isolated from a volcanic region at the Solfatara near Napels [31]. The fumaroles at the Solfatara are characterized by a low pH (down to 1.0), high temperatures (up to 70 °C) and emit 73 t of CH_4 per km^2 per year [31,32]. Physiological studies on SolV have shown that it can grow in extreme conditions, below pH 1 and up to 65 °C [31]. Unlike many Alpha- and Gamma-proteobacteria, SolV fixes carbon via the Calvin-Benson-Bassham cycle [15]. As a nitrogen source it can utilize ammonium, nitrate or dinitrogen gas [31,33]. Like many other methanotrophs, SolV is a nitrifier, oxidizing ammonia to nitrite and a hydrogenotroph [34–37]. The genome of SolV encodes three different copies of the *pmoCAB* operon for methane activation, which are differentially expressed depending on growth conditions [35,38], and no *smo* operon was detected. To oxidize methanol, SolV encodes for a single XoxF-type MDH, encoded by *xoxF*, which is in an operon together with *xoxJ* and a *xoxGJ* fusion in the following order: *xoxF*, *xoxJ*, *xoxGJ* [17,39].

Here we purified and characterized a novel cytochrome c_L homolog fused to an MxaJ homolog (XoxGJ fusion protein) from the thermoacidophilic methanotroph *Methylacidiphilum fumariolicum* SolV. This XoxGJ fusion protein is present in all thermophilic Verrucomicrobia and also in several *Bradyrhizobium* species [21]. We demonstrate its function as an electron acceptor for XoxF-type MDH. Furthermore, we characterized this novel cytochrome c_{GJ} extensively using UV–Vis spectroscopy, electrochemical redox titrations and variable temperature variable field (VTVH) magnetic circular dichroism (MCD) and CD spectroscopy among other methods.

2. Materials and methods

2.1. Cell culture

The batch cultivation of *Methylacidiphilum fumariolicum* SolV was carried out in a 15 l fermenter (Applikon, Delft, The Netherlands). The growth medium consisted of 0.2 mM $MgCl_2$, 1 mM Na_2SO_4, 2 mM K_2SO_4, 4 mM $(NH_4)_2SO_4$, 1 mM NaH_2PO_4. The following trace elements were added from a 10,000 times concentrated stock in 1.5% sulfuric acid: 20 μM $FeSO_4{\cdot}7\ H_2O$, 1 μM $ZnSO_4{\cdot}7\ H_2O$, 1 μM $CoCl_2{\cdot}6\ H_2O$, 20 μM $MnCl_2{\cdot}4\ H_2O$, 30 μM $CuSO_4{\cdot}5\ H_2O$, 1 μM $NiCl_2{\cdot}6\ H_2O$, 1 μM $Na_2MoO_4{\cdot}2\ H_2O$ and 1 μM $CeCl_3{\cdot}7\ H_2O$, which were complexed in the medium with an equimolar amount of nitrilotriacetic acid. These amounts of trace elements were enough to obtain exponential growth to an optical density (600 nm) of 10. The medium was set to pH 2.7 by addition of H_2SO_4 and 0.2 mM $CaCl_2$ was added separately after autoclaving. A gas mixture of 10–50% CH_4 and 5% CO_2 in N_2 was supplied in a continuous flow (50–200 ml/min). The dissolved oxygen concentration was maintained between 5 and 15% oxygen saturation by adding air or oxygen. The pH was kept between 2.5 and 3 through addition of 1 M NaOH. The fermenter was stirred at 1000 rpm and kept at 55 °C.

2.2. Protein purification

Methylacidiphilum fumariolicum SolV cells were harvested by centrifugation at 5000*g* for 15 min. The cell pellet was resuspended in demi water to remove salts and neutralize the pH and centrifuged again. Then the cells were resuspended in 20 mM potassium phosphate pH 7.2 and broken by passing them two times through a French press at 20,000 psi. After removing cell debris and membranes by centrifugation for 1 h at 30,000*g*, the cell-free extract was applied on a SP Sepharose-FF cation exchange column (GE Healthcare; 26 mm × 20 cm) equilibrated with 20 mM potassium phosphate pH 7.2. Proteins were eluted by a seven column volume linear gradient of 0–500 mM NaCl. Fractions containing the bright yellow cytochrome *c* containing XoxG/XoxJ fusion protein (further referred to as cytochrome c_{GJ}), eluting at 50 mM NaCl were pooled and concentrated on a Vivaspin spinfilter (Sartorius) with a 10,000 MW cut-off and reapplied on the same SP-Sepharose column. Proteins were eluted with a ten column volume linear gradient of 0–50 mM NaCl. Bright yellow protein fractions were pooled and concentrated again and applied on a Superdex 75 10/300 GL column (GE Healthcare, 10 mm × 30 cm) equilibrated with 20 mM potassium phosphate 200 mM NaCl pH 7.0. The Superdex 75 column was calibrated with a mixture of 1 mg/ml Dextan Blue, 4 mg/ml conalbumin, 4 mg/ml ovalbumine and 3 mg/ml RNAse A. Pure cytochrome c_{GJ} eluted at a mass of 26 kDa.

2.3. Electrochemical redox titration

Redox titrations of the purified cytochrome c_{GJ} were performed using a homebuilt optically transparent thin-layer electrochemical cell (OTTLE), designed by the workshop of the physical chemistry department of the University of Freiburg as adapted from Baymann et al. [40]. The OTTLE was connected to a potentiostat (PGSTAT204, Metrohm Autolab) and spectroscopic changes were measured using a Cary 60 spectrophotometer (Agilent) in the range of 400 to 700 nm. The Ag/AgCl reference electrode was calibrated with a saturated quinhydrone solution in 1 M MOPS buffer pH 7 ($E^{o'} = +280$ mV) [41]. The assay mixture contained 25 μM cytochrome c_{GJ} in either 50 mM MOPS pH 7 or 20 mM sodium acetate/ acetic acid pH 4, 50 mM KCl, 40 mM glucose, 10 U glucose oxidase, 5 U catalase, 20 μM ferrocene, 20 μM ferricyanide, 20 μM 1,4-benzoquinone, 2,5-dimethyl-1,4-benzoquinone, 1,2-naphtoquinone and 20 μM phenazine methosulfate. Titrations were performed at room temperature. Potential was applied from +50 to +500 mV (vs SHE) in 25 mV steps, in both reductive and oxidative directions. Every 5 min a spectrum was recorded and the potential was

adjusted when no changes where observed (max. 15 min). Spectral changes in the Soret at 440 nm and the α-band at 595 nm were corrected for total spectrum shift by subtracting the absorbance of the closest isosbestic point at 455 nm and 611 nm, respectively. Those absorbance values were normalized and plotted against the potential. The midpoint potentials were determined by fitting the normalized amplitudes to the Nernst equation with one electron component using Origin version 9.1 (OriginLab Corp.).

2.4. Pyridine hemochrome assay

A pyridine hemochrome assay of cytochrome c_{GJ} was performed as previously described by Berry and Trumpower [42]. Purified cytochrome c_{GJ} (2.5 μM) was added to a 1 ml pyridine solution (20% *v*/v pyridine in 0.1 M NaOH) in a 1 cm path length suprasil quartz cuvette. The sample was oxidized by the addition of potassium hexacyanidoferrate(III) after which a spectrum was recorded using a Cary 60 spectrophotometer (Agilent). Afterwards, the sample was reduced by adding an excess of sodium dithionite powder (~2 mg) and another spectrum was recorded. Reduced minus oxidized spectra were used to determine the location the α- and β-bands, 586 and 544 nm respectively.

2.5. Activity assays

Reduction of cytochrome c_{GJ} by XoxF-type MDH (purified according to [17]) was monitored spectroscopically at the Soret band (440 nm) and the α-band (595 nm), using a Cary 60 spectrophotometer (Agilent). 5 μM cytochrome c_{GJ} was incubated in 20 mM potassium phosphate pH 7.0 with 50 μM methanol and 0–300 mM NaCl. After one min, 50 nM XoxF MDH was added and the reaction was followed to the complete reduction of cytochrome c_{GJ}. Assays were performed at 45 °C. To determine the optimal salt concentration of the assay, initial rates were plotted against the respective NaCl concentration.

Reduction of equine or bovine heart cytochrome *c* (Sigma) by cytochrome c_{GJ} and XoxF-type MDH was assayed using the following protocol. 0.2 mM stock solutions of heart cytochromes were prepared fresh in 10 mM PIPES buffer pH 7.2 (1,4-Piperazinediethanesulfonic acid, Sigma) and amber tubes prior to use. Eu-MDH [43] and cytochrome c_{GJ} were washed twice to remove salts and excess methanol by using spin filters (Vivaspin, Sartorius) with 30,000 or 10,000 MW cutoff. Reduction was followed at 45 °C and 550 nm using 96 well microtiter plates and the Epoch2 plate reader (BioTek). Each well contained 200 μl volume and 50 μM equine or bovine heart cytochrome, 0.2 μM Eu-MDH, 0–1 μM cytochrome c_{GJ} and 50 mM Methanol, all in 10 mM PIPES pH 7.2. Control reactions were run without Eu-MDH, methanol or cytochrome c_{GJ} and neither of those showed reduction of the secondary electron acceptors, albeit traces of residual methanol let to a small reduction activity in the absence of excess methanol. To determine the amount of reduced heart cytochrome per minute, an extinction coefficient of 19.5 $mM^{-1}\,cm^{-1}$ at pH 7.2 was determined by subtracting the absorbance of the oxidized form from the fully reduced cytochrome (obtained by addition of 100 equivalents of sodium dithionite, we found the absorption to be both pH and buffer dependent and recommend to determine the extinction coefficient for the used conditions). This extinction coefficient is close to the reported value of 19.0 $mM^{-1}\,cm^{-1}$ at pH 7.0 in 120 mM MOPS buffer [44].

2.6. UV–Vis and CD spectroscopy

The protein was washed with sodium phosphate buffer (20 mM, pH 7) to remove salts, methanol and degraded protein. A spin filter (Vivaspin, Sartorius) with 10,000 MW cutoff was used for this purpose. 200 μl cytochrome c_{GJ} (72 μM) was diluted two times in buffer and the resulting protein solution was centrifuged at 4 °C for 4 min at 4500 rpm with a microclick fixed angle rotor from Heraeus. The flow through was discarded and the procedure repeated once. Then, 200 μl buffer was added and the solution was centrifuged for 8 min. After two subsequent additions of 200 μl buffer the solution was centrifuged for 10 and 15 min, respectively. This procedure yielded approximately 500 μl washed cytochrome c_{GJ} with a concentration of 30 μM which was kept on ice in an amber Eppendorf vial until further use. A 1 mm path length Quartz suprasil cuvette with Teflon stopper was filled with washed cytochrome c_{GJ} and the UV Vis recorded under ambient conditions (air, 25 °C) on a CARY60 spectrophotometer equipped with a xenon flash-lamp. The same cuvette was then immediately transferred to a JASCO CD spectrometer and the spectrum recorded from 190 to 800 nm. CD-Instrument parameters: Data pitch 0.1 nm, Instrument Name J-810-150S, Photometric Mode CD, HT, Sensitivity Standard, D.I.T. 1 s, Bandwidth 1.00 nm, Scanning Speed 500 nm/min, Manual Baseline correction, Accumulation Times 5. To fully reduce the cytochrome c_{GJ} a 100 mM solution of $Na_2S_2O_4$ was added (1.2 μl, 200 equiv.) to a solution of 200 μl washed cytochrome c_{GJ}, and incubated on ice for 5 min. The UV Vis and CD spectra were then immediately recorded of the reduced cytochrome c_{GJ} as described above. To oxidize, a 100 mM solution of $K_3[Fe(CN)_6]$ was added (1.2 μl, 200 equiv.) to a solution of 200 μl washed cytochrome c_{GJ}, and the mixture was incubated on ice for 5 min. The UV Vis and CD spectra were then immediately recorded of the oxidized cytochrome c_{GJ} as described above.

2.7. Extinction coefficient determination

Extinction coefficients were determined from the absorbance values of the Soret and α-band of a 7 μM cytochrome c_{GJ} solution. The protein concentration of purified cytochrome c_{GJ} was determined using the absorbance at 280 nm and an extinction coefficient of 37,275 $M^{-1}cm^{-1}$ determined according to the Edelhoch method [45].

2.8. Metal analysis by ICP-MS

To analyze the iron content, the purified SolV cytochrome c_{GJ} was diluted in 65% nitric acid to a final concentration of 30% and heated at 100 °C for 180 min. After sample preparation, metal analysis was performed using an Inductively Coupled Plasma Mass Spectrometer (ICP-MS; I series, ThermoScientific). Height point calibration was performed with a dilution series of element standards (1000 ppm in 1% nitric acid, Merck). Combined with the absorbance values of the sample, before destruction, at 280 and 430 nm, the iron content of SolV cytochrome c_{GJ} was determined to be 0.99 ± 0.06 mol Fe/mol protein ($n = 4$).

2.9. MCD spectroscopy

Protein samples of cytochrome c_{GJ} were prepared by mixing 400 μl of cytochrome c_{GJ} (72 μM) with 600 μl glycerol and loaded in a 0.62 cm path length nickel-plated copper sample cell with quartz windows. The MCD system used has a JASCO J815 spectropolarimeter and an Oxford Instruments SM4000 cryostat/magnet. Data were collected at increments of 0.5 Tesla (T) from 0 to 7.0 T and at temperatures of 1.5, 4.2, 6, 12, 24 and 48 K. Each spectrum was corrected for any natural CD by subtracting the zero-field spectrum of the sample and in addition by manual baseline correction using the isosbestic points at 352, 430 and 467 nm. The fitting of the VTVH data was achieved with the Fortran software VTVH 2.1.1. [46].

2.10. Mass spectrometry

Sample preparation for matrix assisted laser desorption/ionization time-of-flight mass spectrometry (MALDI-TOF MS) was performed according to Farhoud et al [47]. Briefly, the purified protein was run on SDS-PAGE and stained with Coomassie blue. The protein band was excised and cut into small blocks of 2 × 2 mm. After destaining, reduction and alkylation of cysteines was performed and the gel pieces

Table 1
Properties of the cytochrome c_{GJ} (XoxGJ fusion) of *Methylacidiphilum fumariolicum* SolV.

		Soret				α					
Gene	Protein	Absorbance maximum oxidized (nm)	Absorbance maximum reduced (nm)	$\varepsilon_{433,oxidized}$ ($mM^{-1}cm^{-1}$)	$\varepsilon_{440,reduced}$ ($mM^{-1}cm^{-1}$)	Absorbance maximum (nm)	$\varepsilon_{595,oxidized}$ ($mM^{-1}cm^{-1}$)	$\varepsilon_{595,reduced}$ ($mM^{-1}cm^{-1}$)	$E_{m,7}$ (mV)	$E_{m,4}$ (mV)
Mfumv2_1185	XoxGJ	433	440	60.2	85.4	595	4.9	10.6	240	255

were incubated overnight in a trypsin solution (10 ng/ml trypsin) at 37 °C. Peptides were collected, mixed with an equal volume of 10 mg/ml 4-hydroxy-α-cyanocinnamic acid in 50% acetonitrile/ 0.05% trifluoroacetic acid and spotted onto a 96 wells stainless steel plate. A spectrum in the range of 600 to 3000 *m/z* was recorded using a Microflex LRF MALDI-TOF (Bruker) and analysed using the Mascot Peptide mass Fingerprint against the *Methylacidiphilum fumariolicum* SolV protein database. A peptide tolerance of 0.3 Da, methionine oxidation as a variable modification and one missed trypsin cleavage were allowed.

To determine the mass of the XoxGJ protein, linear mode MALDI-TOF MS using a Microflex LRF MALDI-TOF (Bruker) was performed on the undigested protein. XoxGJ was diluted 10 fold in matrix solution (10 mg/ml 3,5-dimethoxy-4-hydroxycinnamic acid in 50% acetonitrile/ 0.05% trifluoroacetic acid; Sigma). Calibration was performed with a cytochrome *c* (12,361.96 Da) and albumin (66,429.09 Da) standard (Sigma). The mass of XoxGJ was determined by taking the average of the monoisotopic masses found at MH^+, MH_2^+ and M_2H^+, corrected for their respective charge.

2.11. Gel electrophoresis

4–15% SDS polyacrylamide gradient gels (PAGE [48];) were cast using model 475 gradient delivery system (Bio-Rad). Purified cytochrome c_{GJ} was incubated in SDS sample buffer (62.5 mM Tris, 2% SDS, 50 mM TCEP, 10% glycerol, 0.005% bromophenol blue, pH 6.8) for 30 min at 50 °C before being loaded on the gel (CSH Protocols, 2006; doi:https://doi.org/10.1101/pdb.prot4540). After running, the gels were either stained with Coomassie Brilliant Blue or with a luminol based heme stain adapted from Mruk and Cheng [49]. After fixing the gel in 40% ethanol for 10 min it was incubated for 15 min in a luminol solution (5 mg luminol, 2 ml p-hydroxycoumaric acid (1 mg/ml in ethanol), 2 ml 1 M CAPS pH 11, 16 ml ultrapure water) after which 200 µl of 3% H_2O_2 was added. After an additional 5 min incubation, the gel was imaged using ChemiDoc (Bio-Rad) with the chemiluminescence program and an exposure time of 10 s.

3. Results and discussion

3.1. Genomic organization

The MDH operon in *Methylacidiphilum fumariolicum* SolV is organized as follows: *xoxF*, *xoxJ*, *xoxGJ*. This genomic organization is highly conserved in most methanotrophs utilizing either the MxaF- or XoxF-type MDH, of which the former also includes the *mxaI* gene encoding for the MDH small subunit [21]. Remarkable is the presence of a *xoxGJ* fusion, which is so far only present in *Bradyrhizobium* and thermophilic Verrucomicrobia species. Multiple sequence alignments and structural predictions of SolV XoxJ and the XoxJ part of the XoxGJ fusion protein with their MxaJ counterparts showed that although the overall sequence similarity is quite low, a similar fold can be adopted by SolV XoxJ (Fig. S1). The XoxJ part of the XoxGJ fusion is truncated compared to the other sequences and misses some of the secondary structure elements (Fig. S1). MxaJ has been postulated to facilitate the formation of functional complexes either between MDH and pMMO or MDH and MxaG [27]. The presence of a XoxGJ fusion protein would favor the latter role and although not all structural elements were conserved, the fusion of XoxJ with one of its proposed interaction partners, XoxG, a condensed structure might be sufficient for its function. The presence of an additional XoxJ in SolV might indicate separate distinct functions for both proteins, where one facilitates the interaction between MDH and the XoxG to which it is fused, the other facilitates binding of MDH to pMMO. In transcriptome analysis of SolV, both *xoxJ* and *xoxGJ* are expressed in the same order of magnitude for cells growing at μ_{max} [35]. Cells grown under H_2/NH_4 conditions showed a twofold decrease in *xoxJ* expression, following the trend of the

decreased expression for the *pmoCAB2* operon [35]. This suggests that XoxJ is involved in a specific interaction of XoxF with one of the pMMO isoforms. XoxF has been shown to interact with pMMO in *M. buryatense* with a K_D value of 50 μM [50], which is considerably higher than the reported K_D value of 0.9 μM for MxaFI with pMMO in *M. capsulatus* [51].

3.2. Purification of the XoxGJ fusion protein

The gene product of Mfumv2_1185, the cytochrome c_{GJ} XoxGJ fusion protein from *Methylacidiphilum fumariolicum* SolV was purified as a yellowish protein (See Table 1 for an overview of characteristics). SDS-PAGE showed a major protein band with a mass of ~25 kDa (Fig. S2A), in agreement with the mass observed during size exclusion chromatography (~26 kDa), but slightly lower than theoretical mass of ~29 kDa calculated for the XoxJG fusion protein on the basis of the gene sequence without leader peptide. Tryptic digestion of the gel band and analysis of the peptides using MALDI-TOF MS identified the protein as the gene product of Mfumv2_1185, with a Mowse score of 75 and 9 detected peptides resulting in a 31% coverage. A luminol-based heme stain after gel electrophoresis showed a strong signal for the 25 kDa XoxGJ band, suggesting the presence of a covalently attached heme *c* moiety. Using linear mode MALDI-TOF MS on the undigested XoxGJ protein (Fig. S2B), the mass of the protein was determined at 29,746 ± 77 Da, close to the theoretical mass of the polypeptide (signal peptide removed) plus heme *c* of 29,783 Da.

3.3. Spectral characteristics

The spectrum of the cytochrome c_{GJ} directly after purification suggests, due to its similarity to the dithionite reduced spectrum (Fig. 1, black trace), that it is mainly present in the reduced form containing iron(II) (Fig. 1, red trace). However, a small amount of iron(III) is present in the sample and thus a small band arising from the Met-Fe CT transition can be detected at 695 nm (Fig. 1C) [52], in agreement with the presence of a conserved methionine in a multiple sequence alignment of MxaG/XoxG (Fig. S3). It is notable to mention that the protein (washed using a spin filter to remove degraded protein and salts from the purification process) after storage is mainly in its oxidized form (Fig. 1, blue trace).

Interestingly, the spectra that were recorded directly after purification and the ones from the protein that had been stored at −80 °C (independent of oxidation state) differed in that sense that the methionine to Fe^{III} charge transfer transition had disappeared and even upon full oxidation did not reappear. It is likely that the methionine-ligation is lost upon storage. This “MetLoss” [54] behavior is not unusual for cytochromes and has been observed and studied for the cytochromes of *Methylobacterium extorquens* strains *AM1* and many others [25,26,52,54–57]. Upon crystallization of the *Methylobacterium extorquens* cytochrome, the ligation at the iron changed from Met109 to His112, and this was proposed to be due to the high mobility of the loop containing these residues [25]. The same behavior has been demonstrated for cytochrome c_2 isolated from *Rhodopseudomonas palustris,* here the axial methionine ligand is replaced by an ammonia molecule during the crystallization process and this was also attributed to the high flexibility of the methionine-containing loop [56]. The lability of the ligation was further demonstrated for cytochrome c_L from *Methylobacterium extroquens* AM1 which readily reacts with carbon monoxide [26].

The cytochrome c_{GJ} isolated from SolV overall displays an unusual absorbance spectrum. Remarkably, the Soret band of the reduced protein is found at 440 nm, extremely red shifted for a cytochrome c_L. In addition, the quasi-allowed bands are observed at 552 and 595 nm in the reduced form. The absorption bands of the porphyrin ring of cytochrome c_L from *Methylobacterium extorquens* AM1 (found at 549 nm and 416 nm) [25,26] and that from their cytochrome c-553 (553, 419 nm reduced and 414 nm oxidized) [58], are distinctly different to the cytochrome c_{GJ} reported here, pointing towards a modification of or near the heme in the SolV protein. Not surprising is that the CT-band which arises from a methionine residue to iron(III) is not shifted and found at 695 nm as for the other systems (Fig. 1C). A recently reported XoxG homolog showed absorption peaks around 525 and 552 nm after reduction by dithionite [24]. Unfortunately, in this study the location of the Soret band was not reported. Two unusual *c*-type cytochromes, c_{572} and c_{579}, that also show red shifted absorbance spectra were previously purified from iron-oxidizing acidophilic microbial communities. Both cytochromes contained canonical CXXCH heme binding motifs and the authors speculated that the shifted spectra might be caused by oxidation of the porphyrin [59,60]. For the cytochrome *bd* oxidase a similar red-shifted spectrum was observed for one of the *b* hemes, termed b_{595}. This red-shift is likely caused by a glutamate axial ligand of the heme [61]. To examine the effect of the axial ligands on the spectrum of cytochrome c_{GJ}, a pyridine hemochrome assay was performed [42]. Here, the heme ligands are replaced by pyridine molecules to eliminate their effect on the spectrum. The pyridine hemochrome assay of cytochrome c_{GJ} showed an α-band at 586 nm and β-band at 544 nm in the reduced minus oxidized spectrum (Fig. 2). Compared to the α-band of a canonical heme *c* (550 nm), cytochrome c_{GJ} still showed a large red-shift, which cannot be attributed to the axial heme ligands. The location of the α-band at 586 nm resembles that of a heme *a*, suggesting that one of the methyl groups of the porphyrin ring might be oxidized to a formyl group [42], as was suggested for cytochrome c_{579} [59].

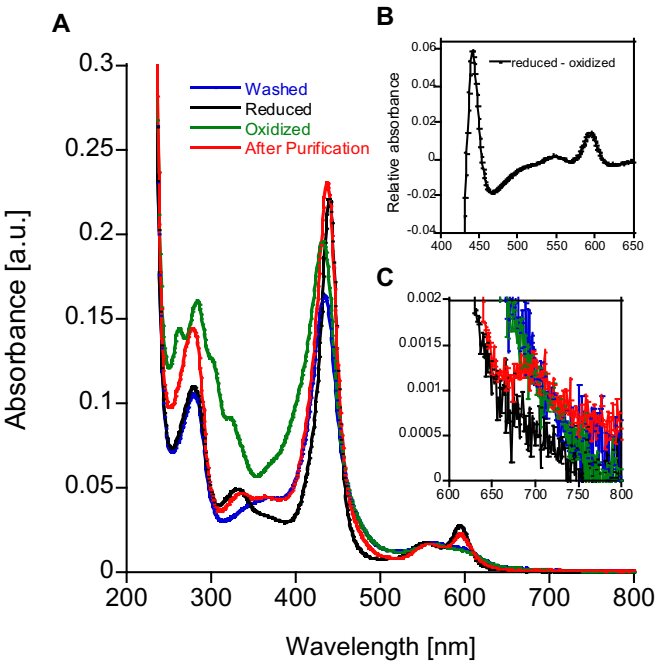

Fig. 1. A: UV–Vis absorbance spectra of washed cytochrome c_{GJ} from *Methylacidiphilum fumariolicum* SolV after storage at −80 °C (blue trace), Quartz suprasil cuvette 1 mm path length, at 30 μM protein concentration, and after addition of 600 μM sodium dithionite (black trace) or potassium hexacyanidoferrate(III) (green trace). Red trace shows the spectrum of the cytochrome recorded immediately after purification and the spectrum has been adjusted to match the intensity of the three other spectra by normalizing the data to 0.22 at 440 nm for better comparison. B: Dithionite reduced minus potassium hexacyanidoferrate(III) oxidized difference spectrum, with absorbance maxima at 441 nm and 595 nm. C: Zoom in of the Met to Fe^{III} CT-band region.

3.4. Electrochemical redox titration

Besides the axial ligands, changes in the absorption spectrum of

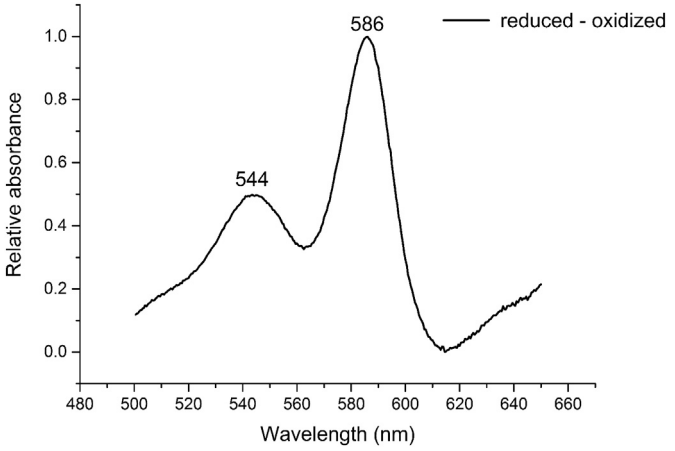

Fig. 2. UV–Vis absorbance spectrum of the pyridine hemochrome of cytochrome c_{GJ} from *Methylacidiphilum fumariolicum* SolV. Cytochrome c_{GJ} was added to 1 ml of pyridine solution (20% *v*/v pyridine in 0.1 M NaOH) in a 1 cm path length Suprasil Quartz cuvette to a 2.5 μM protein concentration. The black trace shows the sodium dithionite reduced minus potassium hexacyanidoferrate(III) oxidized spectrum. The spectrum was normalized to 1 at 586 nm.

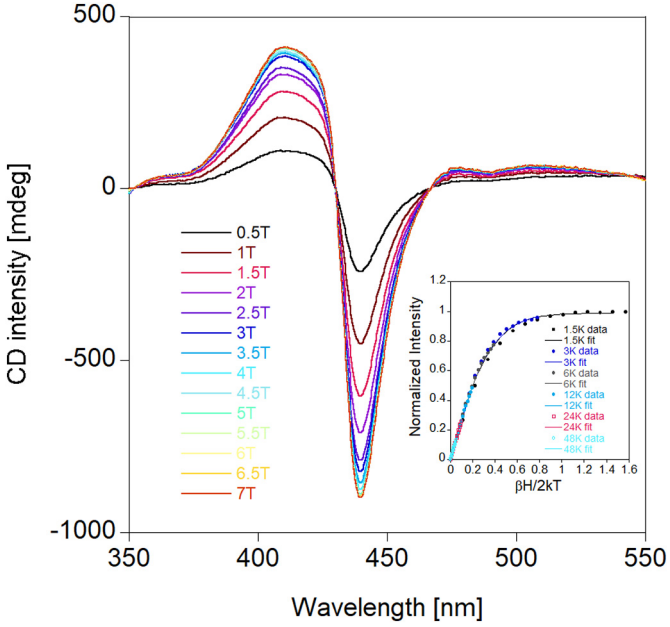

Fig. 4. Variable Field MCD data (baseline corrected) for cytochrome c_{GJ} from *Methylacidiphilum fumariolicum* SolV at 1.5 K in glycerol and buffer at different fields. Inset: Magnetization plots.

hemes can be caused for example by heme distortion or changes in covalent attachment of the cysteine thiol groups. [57,62]. It has been suggested that distortion is one way to tune redox potential and it can either stabilize or destabilize a certain iron redox state and that the more the heme becomes distorted, the lower the reduction potential [63], albeit a clear correlation is lacking. Therefore we performed a spectrophotometric electrochemical redox titration of cytochrome c_{GJ} at pH 7 and pH 4 in the range of +50 to +500 mV versus standard hydrogen electrode. This titration showed that the protein transitions from the completely oxidized to completely reduced form in a 150 mV redox span. Independent fitting of the relative absorbance changes of both the Soret and α-band as a function of the potential, in the reducing and oxidizing direction, using the Nernst equation resulted in a midpoint potential of +240 mV at pH 7 and + 255 mV at pH 4 (Fig. 3). This is similar to the midpoint potential of other cytochrome c_L's at pH 7, which all fall in the range of ~200 mV to ~300 mV [23]. Thus it seems that the heme in SolV cytochrome c_{GJ} is not particularly ruffled, since no effect on the reduction potential is observed. The *Methylobacterium extorquens* AM1 cytochrome c_L showed a strong pH dependence on its midpoint potential, increasing from 250 mV to 320 mV when the pH was dropped from 7 to 4 [26], whereas the SolV cytochrome c_{GJ} was largely unaffected by this pH drop. The heme modification of SolV cytochrome c_{GJ}, might stabilize it at lower pH and prevent the increase in midpoint potential. This would allow the cytochrome to accept electrons from MDH and transfer them (via a second cytochrome) to the terminal oxidase (at ~ 300 mV) as efficiently at acidic as neutral conditions, whereas for *Methylobacterium extorquens* AM1 the increased midpoint potential to a value above that of the terminal oxidase would greatly hamper methanol fueled respiration.

3.5. VTVH-MCD spectroscopy

We further characterized cytochrome c_{GJ} with VTVH-MCD spectroscopy to gain insight into the spin state of the iron center and to detect possible deviations form planarity of the heme ring [64]. MCD spectra of cytochrome c_{GJ} were recorded in a phosphate buffer glycerol mixture at different temperatures ranging from 1.5 K to 48 K and different magnetic fields from 0.5 to 7 T (Fig. 4). The data were baseline corrected for instrument and spectral baseline. As mentioned above, after prolonged storage the iron is in the oxidized form. A full spectrum scan before and after reduction with sodium dithionite and temperature-dependent data at 7 T can be found in the supporting information (Figs. S4 and S5). No major transitions between 600 and 800 nm were

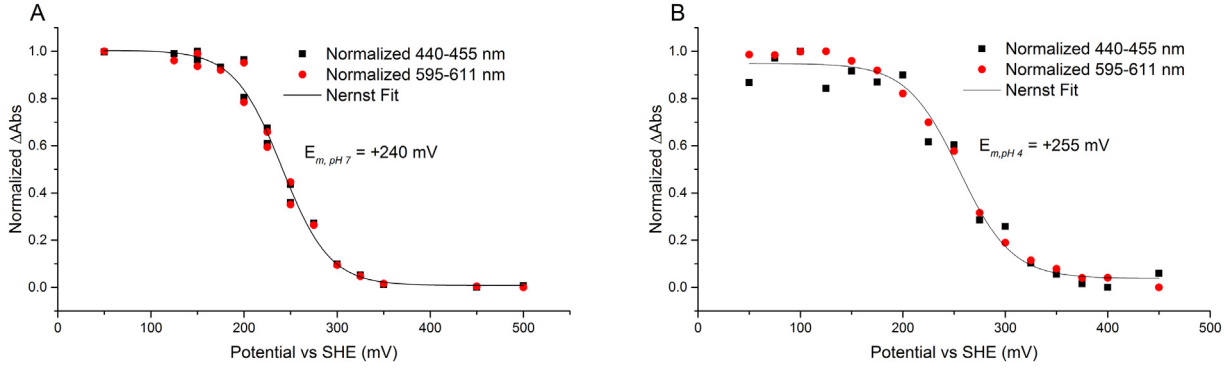

Fig. 3. Spectrophotometric electrochemical redox titration of cytochrome c_{GJ} from *Methylacidiphilum fumariolicum* SolV at pH 7 (A) and at pH 4 (B), both performed at room temperature. The relative absorbance change of the Soret region 440–455 nm (red circles) and α-band 595–611 (black squares) were plotted versus the applied potential vs SHE, measured in both reductive and oxidative direction. The data was fitted to the Nernst equation (black trace), which resulted in one redox transition with a midpoint potential of +240 mV at pH 7 and + 255 mV at pH 4.

observed. The spectra exhibit a large positive temperature-dependent Soret band with a crossover near 430 nm. The intense features in the low temperature MCD spectra are typical for a low spin iron(III) heme [53,65]. The VTVH data were fitted using the Program VTVH 2.0 and the best VTVH-fit was the summed data, where the maximum negative band was subtracted from the maximum positive band, which eliminates baseline correction errors. The fit is consistent with a simple Kramers doublet (S = 1/2) ground state, xy-polarization and g_z contributing the most towards MCD-intensity. There are very small contributions from M_{xz} and M_{yz} as well as g_y and g_x, which is consistent with a small deviation from planarity (i.e. ruffling). This is also in line with the obtained redox potential that did not deviate from the usual range reported for cytochrome c_L. The final values after fit of the Soret band were $g_x = 2.0000$, $g_y = 2.0000$, $g_z = 3.1775$, $M_{xy} = 1.1397$, $M_{xz} = -0.0500$, $M_{yz} = -0.0200$ and a small zero field splitting of $D = -0.0078\ cm^{-1}$.

3.6. Circular dichroism spectroscopy

The washed, oxidized and reduced samples shown above in Fig. 1 were also investigated with circular dichroism spectroscopy to assess integrity during reduction and oxidation. The far UV region spectra shown in Fig. S6 show that protein tertiary structure is minimally affected by the treatment with sodium dithionite or potassium hexacyanidoferrate(III) and the oxidation state [66]. The Soret band feature in the CD, however, is dependent on the oxidation state of the iron with the positive features found at 427 and 420 nm for the reduced and oxidized forms respectively, and the negative features at 442 and 447 nm.

3.7. Physiological role of XoxGJ

The physiological role of cytochrome c_{GJ} from SolV should be the same as that of other cytochrome c_L's i.e. accepting electrons from methanol oxidation by MDH. Hence, to test this function, the reduction state of cytochrome c_{GJ} (5 μM) was followed at 440 nm and 595 nm, the absorbance maxima of the Soret and α- band respectively. After an initial 1 min incubation in the presence of 50 μM methanol to establish a baseline, 50 nM XoxF-type MDH was added (data not shown). MDH catalyzed the rapid oxidation of methanol, shuttling the electrons to cytochrome c_{GJ} as observed by the complete reduction of cytochrome c_{GJ} within minutes. A UV–Vis spectrum of MDH-mediated reduction of cytochrome c_{GJ} can be found in Fig. S7. This demonstrates the direct interaction between MDH and cytochrome c_{GJ}, both isolated from *Methylacidiphilum fumariolicum* SolV, without the need of a small electron carrier such as PMS or PES. Reduction of cytochrome c_L by MDH has already been studied for several methylotrophs utilizing the MxaF-type MDH [23] and has recently been shown for its XoxF-type counterpart [24].

Usually, ionic interactions play a role between the binding of an enzyme to its redox partner and varying salt concentrations can favor binding and dissociation reactions, respectively. To determine the impact of salt concentrations for the MDH cytochrome c_{GJ} couple, initial cytochrome c_{GJ} reduction rates were plotted against NaCl concentration over a range of 0 to 300 mM (Fig. 5). The highest activity was observed at 0 mM NaCl and addition of higher concentrations of salt had an adverse effect on the initial rate until 150 mM NaCl, after which the rate was stabilizing. At low salt concentrations binding of the ferric form is likely optimal. This has been shown for MDH and cytochrome c_L from *Methylobacterium extorquens*, where addition of 50 mM NaCl decreased the affinity of MDH for cytochrome c_L with the K_m value increasing from 3.5 to 31 μM [67]. This indicates that under the tested assay conditions binding of ferric cytochrome c_{GJ} to MDH is the rate-limiting step. In addition to high levels of NaCl, EDTA is also known to inhibit the electron transfer between MDH and cytochrome c_L as shown by Cox et al. [68].

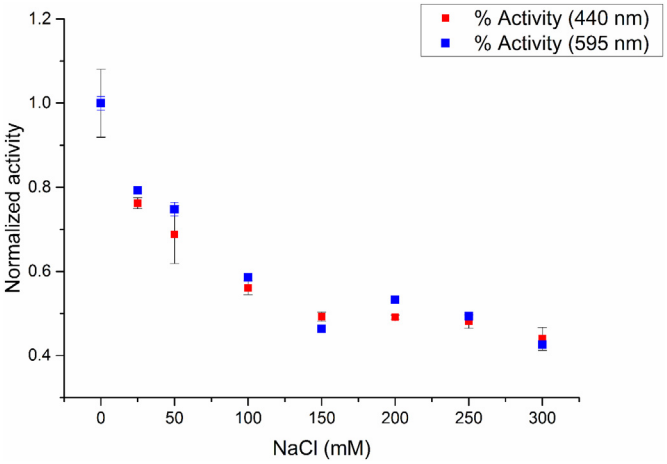

Fig. 5. Effect of salt concentration (0–300 mM NaCl) on the activity of XoxF-type MDH with cytochrome c_{GJ} from *Methylacidiphilum fumariolicum* SolV as electron acceptor. Reduction of cytochrome c_{GJ} (5 μM) was monitored spectroscopically at the Soret (440 nm) and α-band (595 nm), respectively. After an initial 1 min incubation of cytochrome c_{GJ} in 20 mM potassium phosphate pH 7.0 with 50 μM methanol, the reaction was started by the addition of 50 nM XoxF-type MDH. Assays were performed at 45 °C. Activities are shown relative to the maximum activity of the respective wavelength. All datapoints are the means of three measurements and error bars indicate standard deviation.

After electrons are passed from MDH to cytochrome c_L they are transferred to a second cytochrome, cytochrome c_H, which donates its electrons to a terminal oxidase to fuel respiration [23]. Another hypothesis is that methanol oxidation is coupled to methane oxidation either directly or via uphill electron transfer [69]. Metabolic flux analysis on *M. buryatense* showed that the only way to sustain observed growth and methane/oxygen consumption rates, was through the coupling of methanol oxidation to methane oxidation, although the exact mechanism could not be established [70]. In vitro assays however show that, just like reported for *Methylophilus methylotrophus*, *Methylobacterium extorquens* strains and *Acetobacter methanolicus* cytochrome c_L [44,52,68,71], SolV cytochrome c_{GJ} efficiently donates its electrons to a secondary cytochrome (Fig. S8). Both equine and bovine heart cytochrome *c* can be used as secondary electron acceptors to demonstrate this and the reduction of secondary cytochrome is monitored by an increase of absorbance at 550 nm. Increasing the concentration of cytochrome c_{GJ} increased the rate of reduction of equine or bovine horse heart cytochrome *c* with a linear depedence between 0 and 1 μM. For this reduction both cytochrome c_L and MDH are strictly neccesary. A similar pathway for electron flow from methanol oxidation via two cytochromes to a terminal oxidase is thus possible in SolV. Furthermore, methanol addition to crude extract greatly stimulates oxygen consumption in crude cell extracts (data not shown), indicating methanol oxidation can readily fuel respiration.

4. Conclusions

In summary, a novel cytochrome c_L homolog fused to a XoxJ periplasmic binding protein (the product of this fusion is termed here cytochrome c_{GJ}) purified from *Methylacidiphilum fumariolicum* SolV functions as the direct electron acceptor of XoxF-type MDH. To the best of our knowledge, cytochrome c_{GJ} is the first example of a cytochrome from a strictly lanthanide-dependent acidophilic methanotroph. It is readily oxidized by an additional cytochrome partner (e.g. bovine and equine heart cytochrome *c*), indicating it could fuel respiration via a terminal oxidase. Compared to canonical cytochrome *c*'s and specifically previously studied cytochrome c_L's, the SolV fusion protein has a red-shifted absorbance spectrum. This red-shift has also been observed in two cytochromes isolated from acidophilic iron oxidizing microbial

communities. It is possible that a heme-modification stabilizes the cytochrome function at acidic conditions. The midpoint potential of *Methylobacterium extorquens AM1* cytochrome c_L increased by +70 mV when the pH was lowered from 7 to 4, whereas the cytochrome $c_{G,J}$ from SolV was largely unaffected by this pH drop. This would allow SolV cytochrome $c_{G,J}$ to keep functioning under its natural, acidic conditions.

Acknowledgements

WV, JR and MSMJ were supported by ERC AG Ecomom 339880; HJMO was supported by ERCAG VOLCANO 669371. WV was also supported by the Netherlands Organization for Scientific Research [NWO 824.15.011 to BK]. The authors would like to thank Simon Lindhoud for assistance with MALDI-TOF MS analysis. JAL acknowledges the National Science Foundation (USA), grant CHE-0820965 for the MCD instrument. LJD gratefully acknowledges funding from the Deutsche Forschungsgemeinschaft (DFG) – Project number 392552271 and CIPSM as well as Prof. Peter Klüfers for access to the JASCO CD instrument.

Conflict of interest

The authors declare that they have no conflicts of interest with the content of this article.

Appendix A. Supplementary data

Supplementary data to this article can be found online at https://doi.org/10.1016/j.bbapap.2019.04.001.

References

[1] R.K. Thauer, A.K. Kaster, H. Seedorf, W. Buckel, R. Hedderich, Methanogenic archaea: ecologically relevant differences in energy conservation, Nat. Rev. Microbiol. 6 (2008) 579–591, https://doi.org/10.1038/nrmicro1931.
[2] R. Conrad, The global methane cycle: recent advances in understanding the microbial processes involved, Environ. Microbiol. Rep. 1 (2009) 285–292, https://doi.org/10.1111/j.1758-2229.2009.00038.x.
[3] R.S. Hanson, T.E. Hanson, Methanotrophic bacteria, Microbiol. Rev. 60 (1996) 439–471.
[4] O. Rasigraf, D.M. Kool, M.S. Jetten, J.S. Sinninghe Damste, K.F. Ettwig, Autotrophic carbon dioxide fixation via the Calvin-Benson-Bassham cycle by the denitrifying methanotroph "*Candidatus* Methylomirabilis oxyfera", Appl. Environ. Microbiol. 80 (2014) 2451–2460, https://doi.org/10.1128/AEM.04199-13.
[5] Raghoebarsing, A. A., Pol, A., van de Pas-Schoonen, K. T., Smolders, A. J., Ettwig, K. F., Rijpstra, W. I., Schouten, S., Damste, J. S., Op den Camp, H. J. M., Jetten, M. S. M., and Strous, M. (2006) A microbial consortium couples anaerobic methane oxidation to denitrification. Nature 440, 918–921, https://doi.org/10.1038/nature04617.
[6] K.F. Ettwig, B. Zhu, D. Speth, J.T. Keltjens, M.S.M. Jetten, B. Kartal, Archaea catalyze iron-dependent anaerobic oxidation of methane, Proc. Natl. Acad. Sci. U. S. A. 113 (2016) 12792–12796, https://doi.org/10.1073/pnas.1609534113.
[7] M.F. Haroon, S. Hu, Y. Shi, M. Imelfort, J. Keller, P. Hugenholtz, Z. Yuan, G.W. Tyson, Anaerobic oxidation of methane coupled to nitrate reduction in a novel archaeal lineage, Nature 500 (2013) 567–570, https://doi.org/10.1038/nature12375.
[8] K. Knittel, A. Boetius, Anaerobic oxidation of methane: progress with an unknown process, Annu. Rev. Microbiol. 63 (2009) 311–334, https://doi.org/10.1146/annurev.micro.61.080706.093130.
[9] M.H. In't Zandt, A.E.E. de Jong, C.P. Slomp, M.S.M. Jetten, The hunt for the most-wanted chemolithoautotrophic spookmicrobes, FEMS Microbiol. Ecol. 94 (2018), https://doi.org/10.1093/femsec/fiy064.
[10] J.D. Semrau, A.A. DiSpirito, S. Yoon, Methanotrophs and copper, FEMS Microbiol. Rev. 34 (2010) 496–531, https://doi.org/10.1111/j.1574-6976.2010.00212.x.
[11] H.J.M. Op den Camp, T. Islam, M.B. Stott, H.R. Harhangi, A. Hynes, S. Schouten, M.S.M. Jetten, N.-K. Birkeland, A. Pol, P.F. Dunfield, Environmental, genomic and taxonomic perspectives on methanotrophic Verrucomicrobia, Environ. Microbiol. Rep. 1 (2009) 293–306, https://doi.org/10.1111/j.1758-2229.2009.00022.x.
[12] L. Chistoserdova, M.E. Lidstrom, Aerobic methylotrophic prokaryotes, in: E. Rosenberg, E.F. DeLong, S. Lory, E. Stackebrandt, F. Thompson (Eds.), The Prokaryotes: Prokaryotic Physiology and Biochemistry, Springer Berlin Heidelberg, Berlin, Heidelberg, 2013, pp. 267–285.
[13] S. Sirajuddin, A.C. Rosenzweig, Enzymatic oxidation of methane, Biochemistry 54 (2015) 2283–2294, https://doi.org/10.1021/acs.biochem.5b00198.
[14] L. Chistoserdova, Modularity of methylotrophy, revisited, Environ. Microbiol. 13 (2011) 2603–2622, https://doi.org/10.1111/j.1462-2920.2011.02464.x.
[15] A.F. Khadem, A. Pol, A. Wieczorek, S.S. Mohammadi, K.J. Francoijs, H.G. Stunnenberg, M.S. Jetten, H.J.M. Op den Camp, Autotrophic methanotrophy in verrucomicrobia: Methylacidiphilum fumariolicum SolV uses the Calvin-Benson-Bassham cycle for carbon dioxide fixation, J. Bacteriol. 193 (2011) 4438–4446, https://doi.org/10.1128/JB.00407-11.
[16] C. Anthony, Methanol dehydrogenase, a PQQ-containing quinoprotein dehydrogenase, Subcell. Biochem. 35 (2000) 73–117.
[17] A. Pol, T.R.M. Barends, A. Dietl, A.F. Khadem, J. Eygensteyn, M.S.M. Jetten, H.J.M. Op den Camp, Rare earth metals are essential for methanotrophic life in volcanic mudpots, Environ. Microbiol. 16 (2014) 255–264, https://doi.org/10.1111/1462-2920.12249.
[18] T. Nakagawa, R. Mitsui, A. Tani, K. Sasa, S. Tashiro, T. Iwama, T. Hayakawa, K. Kawai, A catalytic role of XoxF1 as La^{3+}-dependent methanol dehydrogenase in Methylobacterium extorquens strain AM1, PLoS One 7 (2012) e50480, , https://doi.org/10.1371/journal.pone.0050480.
[19] Y. Hibi, K. Asai, H. Arafuka, M. Hamajima, T. Iwama, K. Kawai, Molecular structure of La^{3+}-induced methanol dehydrogenase-like protein in *Methylobacterium radiotolerans*, J. Biosci. Bioeng. 111 (2011) 547–549, https://doi.org/10.1016/j.jbiosc.2010.12.017.
[20] N.A. Fitriyanto, M. Fushimi, M. Matsunaga, A. Pertiwiningrum, T. Iwama, K. Kawai, Molecular structure and gene analysis of Ce^{3+} −induced methanol dehydrogenase of *Bradyrhizobium* sp. MAFF211645, J. Biosci. Bioeng. 111 (2011) 613–617, https://doi.org/10.1016/j.jbiosc.2011.01.015.
[21] J.T. Keltjens, A. Pol, J. Reimann, H.J.M. Op den Camp, PQQ-dependent methanol dehydrogenases: rare-earth elements make a difference, Appl. Microbiol. Biotechnol. 98 (2014) 6163–6183, https://doi.org/10.1007/s00253-014-5766-8.
[22] Z. Yu, D.A.C. Beck, L. Chistoserdova, Natural selection in synthetic communities highlights the roles of methylococcaceae and methylophilaceae and suggests differential roles for alternative methanol dehydrogenases in methane consumption, Front. Microbiol. 8 (2392) (2017), https://doi.org/10.3389/fmicb.2017.02392.
[23] C. Anthony, The c-type cytochromes of methylotrophic bacteria, Biochim. Biophys. Acta 1099 (1992) 1–15.
[24] Zheng, Y., Huang, J., Zhao, F., and Chistoserdova, L. (2018) Physiological effect of XoxG(4) on lanthanide-dependent methanotrophy. mBio 9, e02430-02417, https://doi.org/10.1128/mBio.02430-17.
[25] P. Williams, L. Coates, F. Mohammed, R. Gill, P. Erskine, D. Bourgeois, S.P. Wood, C. Anthony, J.B. Cooper, The 1.6 angstrom X-ray structure of the unusual c-type cytochrome, cytochrome c(L), from the methylotrophic bacterium *Methylobacterium extorquens*, J. Mol. Biol. 357 (2006) 151–162, https://doi.org/10.1016/j.jmb.2005.12.055.
[26] D.T. O'Keeffe, C. Anthony, The two cytochromes c in the facultative methylotroph *Pseudomonas* AM1, Biochem. J. 192 (1980) 411–419.
[27] J.M. Choi, T.P. Cao, S.W. Kim, K.H. Lee, S.H. Lee, MxaJ structure reveals a periplasmic binding protein-like architecture with unique secondary structural elements, Proteins 85 (2017) 1379–1386.
[28] R.J. Van Spanning, C.W. Wansell, T. De Boer, M.J. Hazelaar, H. Anazawa, N. Harms, L.F. Oltmann, A.H. Stouthamer, Isolation and characterization of the *moxJ*, *moxG*, *moxI*, and *moxR* genes of *Paracoccus denitrificans*: inactivation of *moxJ*, *moxG*, and *moxR* and the resultant effect on methylotrophic growth, J. Bacteriol. 173 (1991) 6948–6961.
[29] K. Matsushita, K. Takahashi, O. Adachi, A novel quinoprotein methanol dehydrogenase containing an additional 32-kilodalton peptide purified from *Acetobacter methanolicus*: identification of the peptide as a MoxJ product, Biochemistry 32 (1993) 5576–5582.
[30] H.G. Kim, G.H. Han, D. Kim, J.S. Choi, S.W. Kim, Comparative analysis of two types of methanol dehydrogenase from *Methylophaga aminisulfidivorans* MPT grown on methanol, J. Basic Microbiol. 52 (2012) 141–149, https://doi.org/10.1002/jobm.201000479.
[31] A. Pol, K. Heijmans, H.R. Harhangi, D. Tedesco, M.S. Jetten, H.J.M. Op den Camp, Methanotrophy below pH 1 by a new Verrucomicrobia species, Nature 450 (2007) 874–878, https://doi.org/10.1038/nature06222.
[32] S. Castaldi, D. Tedesco, Methane production and consumption in an active volcanic environment of Southern Italy, Chemosphere 58 (2005) 131–139, https://doi.org/10.1016/j.chemosphere.2004.08.023.
[33] A.F. Khadem, A. Pol, M.S.M. Jetten, H.J.M. Op den Camp, Nitrogen fixation by the verrucomicrobial methanotroph '*Methylacidiphilum fumariolicum*' SolV, Microbiology 156 (2010) 1052–1059, https://doi.org/10.1099/mic.0.036061-0.
[34] G. Nyerges, L.Y. Stein, Ammonia cometabolism and product inhibition vary considerably among species of methanotrophic bacteria, FEMS Microbiol. Lett. 297 (2009) 131–136, https://doi.org/10.1111/j.1574-6968.2009.01674.x.
[35] S.S. Mohammadi, A. Pol, T. van Alen, M.S.M. Jetten, H.J.M. Op den Camp, Ammonia oxidation and nitrite reduction in the verrucomicrobial methanotroph *Methylacidiphilum fumariolicum* SolV, Front. Microbiol. 8 (1901) (2017), https://doi.org/10.3389/fmicb.2017.01901.
[36] C. Bedard, R. Knowles, Physiology, biochemistry, and specific inhibitors of CH4, NH^{4+}, and CO oxidation by methanotrophs and nitrifiers, Microbiol. Rev. 53 (1989) 68–84.
[37] S. Mohammadi, A. Pol, T.A. van Alen, M.S.M. Jetten, H.J.M. Op den Camp, *Methylacidiphilum fumariolicum* SolV, a thermoacidophilic 'Knallgas' methanotroph with both an oxygen-sensitive and -insensitive hydrogenase, ISME J. 11 (2017) 945–958, https://doi.org/10.1038/ismej.2016.171.
[38] A.F. Khadem, A. Pol, A.S. Wieczorek, M.S.M. Jetten, H.J.M. Op den Camp, Metabolic regulation of "*Ca.* Methylacidiphilum fumariolicum" SolV cells grown under different nitrogen and oxygen limitations, Front. Microbiol. 3 (266) (2012), https://doi.org/10.3389/fmicb.2012.00266.
[39] S.Y. Anvar, J. Frank, A. Pol, A. Schmitz, K. Kraaijeveld, J.T. den Dunnen, H.J.M. Op

den Camp, The genomic landscape of the verrucomicrobial methanotroph *Methylacidiphilum fumariolicum* SolV, BMC Genomics 15 (2014) 914, https://doi.org/10.1186/1471-2164-15-914.
[40] F. Baymann, D.A. Moss, W. Mantele, An electrochemical assay for the characterization of redox proteins from biological electron transfer chains, Anal. Biochem. 199 (1991) 269–274.
[41] D.A. Moffet, J. Foley, M.H. Hecht, Midpoint reduction potentials and heme binding stoichiometries of de novo proteins from designed combinatorial libraries, Biophys. Chem. 105 (2003) 231–239.
[42] E.A. Berry, B.L. Trumpower, Simultaneous determination of hemes a, b, and c from pyridine hemochrome spectra, Anal. Biochem. 161 (1987) 1–15.
[43] B. Jahn, A. Pol, H. Lumpe, T.R.M. Barends, A. Dietl, C. Hogendoorn, H.J.M. Op den Camp, L.J. Daumann, Similar but not the same: first kinetic and structural analyses of a methanol dehydrogenase containing a Europium ion in the active site, Chembiochem (2018), https://doi.org/10.1002/cbic.201800130.
[44] D.J. Day, C. Anthony, Methanol dehydrogenase from *Methylobacterium extorquens* AM1, Methods in Enzymology, 1990, pp. 210–216.
[45] C.N. Pace, F. Vajdos, L. Fee, G. Grimsley, T. Gray, How to measure and predict the molar absorption coefficient of a protein, Protein Sci. 4 (1995) 2411–2423, https://doi.org/10.1002/pro.5560041120.
[46] M.J. Riley, VTVH 2.1.1 Program for the Simulation and Fitting Variable Temperature - Variable Field MCD Spectra, (2008).
[47] M.H. Farhoud, H.J. Wessels, P.J. Steenbakkers, S. Mattijssen, R.A. Wevers, B.G. van Engelen, M.S.M. Jetten, J.A. Smeitink, L.P. van den Heuvel, J.T. Keltjens, Protein complexes in the archaeon *Methanothermobacter thermautotrophicus* analyzed by blue native/SDS-PAGE and mass spectrometry, Mol. Cell. Proteomics 4 (2005) 1653–1663, https://doi.org/10.1074/mcp.M500171-MCP200.
[48] U.K. Laemmli, Cleavage of structural proteins during the assembly of the head of bacteriophage T4, Nature 227 (1970) 680–685.
[49] D.D. Mruk, C.Y. Cheng, Enhanced chemiluminescence (ECL) for routine immunoblotting: an inexpensive alternative to commercially available kits, Spermatogenesis 1 (2011) 121–122, https://doi.org/10.4161/spmg.1.2.16606.
[50] Y.W. Deng, S.Y. Ro, A.C. Rosenzweig, Structure and function of the lanthanide-dependent methanol dehydrogenase XoxF from the methanotroph *Methylomicrobium buryatense* 5GB1C, J. Biol. Inorg. Chem. 23 (2018) 1037–1047, https://doi.org/10.1007/s00775-018-1604-2.
[51] M.A. Culpepper, A.C. Rosenzweig, Structure and protein-protein interactions of methanol dehydrogenase from *Methylococcus capsulatus* (Bath), Biochemistry 53 (2014) 6211–6219, https://doi.org/10.1021/bi500850j.
[52] M. Beardmore-Gray, D.T. O'Keeffe, C. Anthony, The autoreducible cytochromes c of the methylotrophs *Methylophilus methylotrophus* and *Pseudomonas* AM1, Biochem. J. 207 (1982) 161–165.
[53] M.R. Cheesman, P.J. Little, B.C. Berks, Novel heme ligation in a c-type cytochrome involved in thiosulfate oxidation: EPR and MCD of SoxAX from *Rhodovulum sulfidophilum*, Biochemistry 40 (2001) 10562–10569.
[54] B.D. Levin, K.A. Walsh, K.K. Sullivan, K.L. Bren, S.J. Elliott, Methionine ligand lability of homologous monoheme cytochromes c, Inorg. Chem. 54 (2015) 38–46, https://doi.org/10.1021/ic501186h.
[55] G.W. Pettigrew, R.G. Bartsch, T.E. Meyer, M.D. Kamen, Redox potentials of photosynthetic bacterial cytochromes-C2 and structural bases for variability, Biochim. Biophys. Acta 503 (1978) 509–523, https://doi.org/10.1016/0005-2728(78)90150-0.
[56] S. Geremia, G. Garau, L. Vaccari, R. Sgarra, M.S. Viezzoli, M. Calligaris, L. Randaccio, Cleavage of the iron-methionine bond in c-type cytochromes: crystal structure of oxidized and reduced cytochrome c(2) from Rhodopseudomonas palustris and its ammonia complex, Protein Sci. 11 (2002) 6–17.
[57] K.L. Bren, NMR spectroscopy of paramagnetic heme proteins, Curr. Inorg. Chem. 2 (2012) 273–291.
[58] D.J. Day, D.N. Nunn, C. Anthony, Characterization of a novel soluble c-type cytochrome in a moxD mutant of *Methylobacterium extorquens* AM1, J. Gen. Microbiol. 136 (1990) 181–188, https://doi.org/10.1099/00221287-136-1-181.
[59] S.W. Singer, C.S. Chan, A. Zemla, N.C. VerBerkmoes, M. Hwang, R.L. Hettich, J.F. Banfield, M.P. Thelen, Characterization of cytochrome 579, an unusual cytochrome isolated from an iron-oxidizing microbial community, Appl. Environ. Microbiol. 74 (2008) 4454–4462, https://doi.org/10.1128/Aem.02799-07.
[60] C. Jeans, S.W. Singer, C.S. Chan, N.C. Verberkmoes, M. Shah, R.L. Hettich, J.F. Banfield, M.P. Thelen, Cytochrome 572 is a conspicuous membrane protein with iron oxidation activity purified directly from a natural acidophilic microbial community, ISME J. 2 (2008) 542–550, https://doi.org/10.1038/ismej.2008.17.
[61] S. Safarian, C. Rajendran, H. Muller, J. Preu, J.D. Langer, S. Ovchinnikov, T. Hirose, T. Kusumoto, J. Sakamoto, H. Michel, Structure of a bd oxidase indicates similar mechanisms for membrane-integrated oxygen reductases, Science 352 (2016) 583–586, https://doi.org/10.1126/science.aaf2477.
[62] L. Chen, R.C. Durley, F.S. Mathews, V.L. Davidson, Structure of an electron transfer complex: methylamine dehydrogenase, amicyanin, and cytochrome c551i, Science 264 (1994) 86–90.
[63] S.E. Bowman, K.L. Bren, The chemistry and biochemistry of heme c: functional bases for covalent attachment, Nat. Prod. Rep. 25 (2008) 1118–1130, https://doi.org/10.1039/b717196j.
[64] W.R. Mason, Magnetic Circular Diochroism Spectroscopy, John Wiley and Sons, 2007.
[65] F. Zhong, G.P. Lisi, D.P. Collins, J.H. Dawson, E.V. Pletneva, Redox-dependent stability, protonation, and reactivity of cysteine-bound heme proteins, Proc. Natl. Acad. Sci. U. S. A. 111 (2014) E306–E315, https://doi.org/10.1073/pnas.1317173111.
[66] Y.P. Myer, Conformation of cytochromes. II. Comparative study of circular dichroism spectra, optical rotatory dispersion, and absorption spectra of horse heart cytochrome c, J. Biol. Chem. 243 (1968) 2115–2122.
[67] S.L. Dales, C. Anthony, The interaction of methanol dehydrogenase and its cytochrome electron acceptor, Biochem. J. 312 (1995) 261–265.
[68] J.M. Cox, D.J. Day, C. Anthony, The interaction of methanol dehydrogenase and its electron acceptor, cytochrome c_L in methylotrophic bacteria, Biochim. Biophys. Acta 1119 (1992) 97–106.
[69] D.J. Leak, H. Dalton, Growth yields of methanotrophs .2. A theoretical-analysis, Appl. Microbiol. Biotechnol. 23 (1986) 477–481.
[70] A. de la Torre, A. Metivier, F. Chu, L.M. Laurens, D.A. Beck, P.T. Pienkos, M.E. Lidstrom, M.G. Kalyuzhnaya, Genome-scale metabolic reconstructions and theoretical investigation of methane conversion in *Methylomicrobium buryatense* strain 5G(B1), Microb. Cell Factories 14 (188) (2015), https://doi.org/10.1186/s12934-015-0377-3.
[71] H.T. Chan, C. Anthony, The interaction of methanol dehydrogenase and cytochrome c_L in the acidophilic methylotroph *Acetobacter methanolicus*, Biochem. J. 280 (1991) 139–146.